ACADEMIC PRESS

Available online at www.sciencedirect.com
SCIENCE DIRECT®

Journal of Catalysis 214 (2003) 100–112

JOURNAL OF CATALYSIS

www.elsevier.com/locate/jcat

Relations between structure and catalytic activity of Ce-In-ZSM-5 catalysts for the selective reduction of NO by methane I. The In-ZSM-5 system

T. Sowade,[a] C. Schmidt,[a] F.-W. Schütze,[b,1] H. Berndt,[b] and W. Grünert [a,*]

[a] *Lehrstuhl Technische Chemie, Ruhr-Universität Bochum, D-44780 Bochum, Germany*
[b] *Institut für Angewandte Chemie Berlin-Adlershof, Richard-Willstätter-Straße 12, D-12489 Berlin, Germany*

Received 6 June 2002; revised 24 September 2002; accepted 24 September 2002

Abstract

In-ZSM-5 catalysts for the selective catalytic reduction (SCR) of NO by methane have been prepared by different routes (aqueous ion exchange at different pH values; solid-state ion exchange, sublimation, and transport reaction, with an $InCl_3$ indium source) and compared with respect to their catalytic behavior in the SCR (1000 ppm NO, 1000 ppm methane, 2% O_2 in He, at 30,000 h^{-1}) to elucidate the origin of differing NO conversion-temperature characteristics observed with the In-ZSM-5 catalyst system. The samples were categorized into those containing intrazeolite indium oxo species exclusively or coexisting with extrazeolite indium oxo aggregates, and materials containing exclusively intrazeolite InO_xCl_y species on the basis of structural information available from EXAFS and XPS studies. In addition, physical mixtures of $In(OH)_3$ and NH_4-ZSM-5 were studied. The results confirm that intrazeolite indium oxo species are active SCR sites. Their catalytic properties depend on details of the coordination environment. The presence of extrazeolite InO_x species is hardly reflected in the SCR activity but induces unselective methane activation. The complete failure of an In-silicalite-1 catalyst in NO reduction despite considerable methane activation capability indicates a crucial role of Brønsted acidity for the SCR over In-ZSM-5 catalysts. Intrazeolite InO_xCl_y species exhibit low NO reduction activity, but are able to activate methane as well. With physical mixtures of In_2O_3 and H-ZSM-5 (ex $In(OH)_3$/NH_4-ZSM-5) activities comparable to those of In-ZSM-5 prepared by aqueous techniques were measured. These activities were obtained only when the constituents were well mixed in the catalyst pellets, while segregation in separate pellets strongly decreased the NO conversions.

Keywords: SCR; Methane; In-ZSM-5; Active sites

1. Introduction

The selective catalytic reduction of nitric oxides by hydrocarbons (HC-SCR) has been the focus of environmental catalysis over several years because it bears the promise of an elegant NO_x abatement technology for oxidizing exhaust gases of mobile and stationary sources. A large number of new catalysts have been found in the past decade (reviewed, e.g., in [1–3]), but until now it has not been possible to achieve both high catalytic activity and durability in realistic feeds containing water and SO_2. Development of successful catalyst should be strongly favored by knowledge about the catalyst structure and its relation to the catalytic properties. There has been much effort to collect such information for the more popular catalyst systems, e.g., Cu-ZSM-5, Co-ZSM-5, Fe-ZSM-5 [1–8].

Much less information about catalyst structure and its relation to SCR performance is available for catalysts based on the active component indium. Indium belongs to the few elements able to activate the relatively inert methane reductant. It has been extensively studied as an active component in zeolite systems [9–15], but interesting activities, though with propane and propene reductants, have been also reported for alumina-based materials prepared by impregnation or sol–gel techniques [16,17]. The most notable property of indium zeolite catalysts is, however, their favorable response to pro-

* Corresponding author.
E-mail address: w.gruenert@techem.ruhr-uni-bochum.de (W. Grünert).
[1] Present address: OMG AG&Co KG, dmc^2 Division Automotive Catalysts, D-63403 Hanau, Germany

0021-9517/03/$ – see front matter
doi:10.1016/S0021-9517(02)00076-3

motion by a third component, e.g., noble metals [18–20], Fe_2O_3 [21], cobalt [22], or CeO_2 [23–25]. Promoted In zeolites have been reported to achieve excellent NO conversions in dry feed with both methane and short alkane reductants, and the poisoning effect of water, which is rather strong with unpromoted catalysts, is significantly diminished and almost absent at temperatures $\geqslant 800$ K [18–20,23–25]. According to the literature, intrazeolite indium is attached to zeolite cation sites as InO^+ species, which has been demonstrated by temperature-programmed reduction with CO [24], and this cation has been proposed to be the active SCR site [10,11,13]. However, different preparation routes for In zeolites may result in the presence of different In species, among them extrazeolite moieties, which may also contribute to the SCR activity observed. As to the function of the promoting elements, it has been proposed that they catalyze the oxidation of NO to NO_2, which is a step of the reaction network on these catalysts, more efficiently than the unpromoted In zeolites [18–20]. The CeO_2 promoter has been also found to be an active catalyst for NO oxidation, but it can additionally activate methane (in CeO_2/H-ZSM-5 catalysts [26]).

The present paper aims at the elucidation of the active sites in Ce-In-ZSM-5 catalysts and the identification of their role in the SCR of NO by methane. The first part will deal with the basic In-ZSM-5 system while the second part will extend to the interaction between this system and the Ce promoter [27]. The conclusions will be derived by combining the results of catalytic studies with evidence from the physicochemical characterization of the catalysts by various techniques, in particular EXAFS and XPS. The latter information will be partly cited from a comprehensive study of the relations between the preparation method and the microstructure of indium in In-ZSM-5 catalysts, which has been published recently by some of the present authors [28].

2. Experimental

2.1. Materials

The ZSM-5 zeolite employed was provided by Alsi Penta (NH_4-ZSM-5, "SM 27," Si/Al $\approx$ 14). Indium was applied in aqueous solutions of $In(NO_3)_3$ (Fluka) or as $InCl_3$ (ChemPUR, 99.99%). Despite its hygroscopicity, the latter was used without particular protection from the ambient atmosphere except if stated otherwise. $In(OH)_3$ was obtained from an $In(NO_3)_3$ solution by precipitation with aqueous ammonia (25%). The precipitate was washed in water and dried at 395 K.

A variety of In-ZSM-5 catalysts were prepared by ion exchange, by precipitation, by mechanical mixing, and by dry techniques based on the use of $InCl_3$: solid-state ion exchange, sublimation, and transport reaction. Except for those made via transport reaction, the preparation of these materials has been described in detail in Ref. [28] and will be only briefly summarized here. The codes used to denote the samples are compiled in Table 1. The indium contents reported were determined from X-ray absorption spectra as described in [28].

For ion exchange, a total of 5 g of NH_4-ZSM-5 was suspended in 400 ml of an $In(NO_3)_3$ solution (13 mmol/l) and stirred overnight at room temperature. The initial pH of the $In(NO_3)_3$ solution was set to 6, 2.5, or 1.5 by adding HNO_3, but some results from preparations with uncontrolled initial pH will be given as well. After filtration, the exchange was repeated twice. Subsequently, the material was washed with water and dried at 393 K. These samples will be labeled by **IE** (pH 6), **IE** (pH 2.5), **IE** (pH 1.5), and **IE** (pH nat) (natural pH $\approx$ 6.5, and therefore sensitive to fluctuations in the experimental conditions).

For precipitation, a total of 2 g of H-ZSM-5 was suspended in 100 ml of an $In(NO_3)_3$ solution containing the desired amount of indium, and the precipitation was performed by adding 20 ml aqueous ammonia (25%). The samples were washed with water, dried at 393 K, and calcined in helium at 873 K (heating protocol—2 K/min to 393 K, 5 K/min to 873 K, 2 h isothermal). This sample will be referred to as **P(H)**, indicating that indium was precipitated onto the H-form. A sample in which additional indium was precipitated onto **IE** (pH nat), will be labeled **IE-P**.

For solid-state ion exchange, $InCl_3$ was intimately mixed with dehydrated H-ZSM-5, transferred to a vacuum vessel, and evacuated under a temperature regime including a 5 K/min ramp from room temperature to 873 K and a 2-h isothermal period at this temperature. The samples, which will be labeled **SSIE** (in bold, to differentiate them from the abbreviation of the technique, SSIE; cf. Table 1), were studied after cooling and exposure to air. In one case, an **SSIE** sample was washed in water (1000 ml for 2 g catalyst) to achieve the hydrolysis of the In–Cl bonds in the sample prior to catalysis. $AgNO_3$ tests rendered the washing water hazy even at the end of the washing step; i.e., chloride was still left in the samples. Other pretreatments performed with the same intention will be described in the text.

Sublimation of $InCl_3$ onto dehydrated H-ZSM-5 was performed in flowing nitrogen under the same temperature regime as in the case of procedure SSIE. Since there was no contact between $InCl_3$ and the zeolite in the sublimation apparatus, only volatile indium species had access to the zeolite. Moreover, since the indium fixation on the catalyst gives rise to reaction zones in the fixed bed of the catalyst, the preparation had to be continued up to maximum In loading. The sublimation sample will be labeled **S**. The results presented in [28] show that the structure and stability of the indium species formed were primarily determined by the indium content, not so much by the difference in the preparation procedures.

The transport reaction between MFI materials and anhydrous $InCl_3$ was performed in evacuated glass ampoules at temperatures significantly lower than with solid-state ion exchange or sublimation. The porous support was dehydrated

Table 1
Description of In-ZSM-5 samples

Code	Preparation	wt% In	Structure of indium component, [28]
	(a) Preparations via ion exchange, precipitation and dry methods		
IE (pH 6)	Aqueous ion exchange, initial pH 6	1.1	Extrazeolite + intrazeolite indium[a]
IE (pH 2.5)	Aqueous ion exchange, initial pH between 2 and 3	0.25	Indium exclusively intrazeolite, coordination different from **IE** (pH 6)[a]
IE (pH 1.5)	Aqueous ion exchange, initial pH between 1 and 2	0.17	Indium exclusively intrazeolite, coordination unknown
IE (pH nat)	Aqueous ion exchange without pH control	1.1	Extrazeolite + intrazeolite indium (as in **IE** (pH 6))[a]
IE + **P**	**IE** (nat pH), with InO_x precipitated subsequently	3.9	Extrazeolite + intrazeolite indium (as in **IE** (pH 6))[a]
P(H)	H-ZSM-5 suspended in indium nitrate solution, immediate precipitation with ammonia	7	Extrazeolite + intrazeolite indium[a,b]
SSIE(1)	Mixing $InCl_3$ with H-ZSM-5, heating in vacuo	1.0	Indium exclusively intrazeolite, ≈3.5 O at 2.16 Å/≈2.5 Cl at 2.36 Å
SSIE(2)	Mixing $InCl_3$ with H-ZSM-5, heating in vacuo	2.1	
SSIE(3)	Mixing $InCl_3$ with H-ZSM-5, heating in vacuo	3.2	
SSIE(4)	Mixing $InCl_3$ with H-ZSM-5, heating in vacuo	4.4	
SSIE(4)/W	SSIE(4) washed in water (1 l for 2 g)	4.4	
	Sublimation		
S	Sublimation of $InCl_3$ into H-ZSM-5 in flowing N_2	11.8	As after SSIE
	Transport reaction		
T-Z	Transport reaction $InCl_3$//H-ZSM-5 at 673 K	0.38	–
T-Sil	Transport reaction $InCl_3$//Silicalite-1 at 673 K	1.5	–
	(b) Mechanical mixtures (7 wt% indium in all cases)		
$\mathbf{MM}_{N,Hy}$	NH_4-ZSM-5 and $In(OH)_3$ ground together in a mortar and pelletized		
$\mathbf{MM}_{H,O}$	H-ZSM-5 and In_2O_3 ground together in a mortar and pelletized		
$\mathbf{MM}_{N,Hy}$ (A)	NH_4-ZSM-5 and $In(OH)_3$ pressed into *separate pellets*, mixing of the pellets		
$\mathbf{MM}_{N,Hy}$ (B)	Performing the standard activation treatment (He, 873 K) with $\mathbf{MM}_{N,Hy}$ (A), then grinding the pellets together in a mortar and repelletizing the mixture		
$\mathbf{MM}_{N,Hy}$ (C)	NH_4-ZSM-5 and $In(OH)_3$ ground together in a mortar and pelletized (as $\mathbf{MM}_{N,Hy}$, but different batch)		

[a] For details see text.
[b] After thermal activation in He additional intrazeolite indium, possibly isolated and oligomeric clusters [28].

in the ampoule by thermoevacuation. Subsequently, $InCl_3$ was filled in under a controlled atmosphere (glove box) separated from the support by glass wool. The ampoules were then evacuated, melted off, and held at 673 K in a muffle furnace for 3 days. ZSM-5 and silicalite-1 were employed as porous matrices, and the corresponding In-modified samples will be denoted as **T-Z** and **T-Sil**.

Mechanical mixtures were usually prepared by grinding the zeolite (H or NH_4 form) together with the indium source (In_2O_3 or $In(OH)_3$). Catalysts obtained from this mixture by standard pelletizing (compacting, crushing, and sieving) were used in the catalytic runs, which commenced with thermal activation in flowing He (vide infra). The indium content was 7 wt% in all cases. A different procedure was chosen to investigate the influence of the proximity between the indium an the zeolite component: In this case, $In(OH)_3$ and NH_4-ZSM-5 were pelletized separately and mixed in pelletized form. This state of a "segregated mixture" will be referred to as state A (cf. Table 1). After the standard thermal activation in He (vide infra), a part of this mixture was ground and repelletized, which resulted in a state where the already activated components were remixed (B). The results from these catalysts will be compared with those of a standard mixture (i.e., mixing and pelletizing $In(OH)_3$ and NH_4-ZSM-5, state C). The mixtures will be labeled **MM**, with indices indicating the form of the ZSM-5 used (H for H form and N for NH_4 form) and the indium source (O—oxide, Hy—hydroxide); see Table 1.

2.2. Methods

XP spectra were measured with a Leybold LH 10 spectrometer equipped with an EA 10/100 multichannel detector (Specs) using Mg-K_α excitation (1253.6 eV, 10 kV × 20 mA). The samples were studied after contact with the atmosphere. The binding-energy (BE) scale was referenced to the Si($2p$) line as an internal standard (Si($2p$) = 103.0 V). Elemental ratios in the XPS sampling region were evaluated from line intensity ratios using sensitivity factors given in Ref. [29].

X-ray absorption spectra (InK edge at 27.94 keV) in transmission mode were collected at the Hasylab X1 station (Hamburg) using a Si(311) double crystal monochromator (exclusion of higher harmonics by detuning to 70% maximum intensity). Samples were measured at liquid nitrogen temperature (77 K); the spectrum of an In metal foil was

recorded at the same time (between the second and a third ionization chamber) for energy calibration. The catalysts were diluted with polyethylene, pressed into discs of suitable thickness, and stored in the ambient atmosphere. Hygroscopic reference materials (anhydrous $InCl_3$, In_2O_3) were handled in a glove box and filled into sealable sample compartments between kapton windows.

Data reduction of experimental XAFS was performed with standard procedures described, e.g., in [30,31], which are implemented in the software package WinXAS2.0 [32]. They include pre-edge background subtraction and XANES normalization (linear polynomial for the pre-edge region, 3rd order polynomial for post-edge region, smooth atomic background ($\mu_0(k)$) via cubic splines). The radial distribution function FT[$k^3\chi(k)$] was evaluated by Fourier transformation into the R space of the k^3-weighted experimental function $\chi(k) = (\mu(k) - \mu_0(k))/\mu_0(k)$ multiplied by a Bessel window. For the determination of structural parameters the FEFF7 analysis package [33] was used. To minimize the number of free parameters, equal backscatters were fitted with the same E_0-shift wherever possible and with a similar Debye–Waller factor by varying only the Debye temperature.

Temperature-programmed reduction was carried out with a mixture containing 5.2 vol% H_2 in Ar (50 ml/min), with a 10 K/min temperature ramp between room temperature and 1073 K. The samples, which were studied after catalysis, were previously calcined in air at 873 K (1 h, heating ramp 10 K/min). The hydrogen content of the effluent was measured by a catharometer.

2.3. Catalysis

The SCR of NO with methane was carried out in a catalytic microflow reactor at temperatures between 873 and 523 K. The catalyst (ca. 300 mg, depending on the catalyst density, 250–350 µm) was initially heated in flowing He to 873 K at 5 K/min and kept at this temperature for 1 h. A feed mixture of 1000 ppm NO, 1000 ppm methane, and 2% O_2 in He was then charged to the catalyst at a flow rate of 220 ml/min, which resulted in a GHSV of 30,000 h^{-1}. In some experiments, the feed was moistened by 2 vol% H_2O. The products were analyzed by a combination of gas chromatography (O_2, N_2, CH_4), calibrated mass spectrometry (NO, CH_4, (NO_2)), and calibrated nondispersive IR photometry (CO, CO_2, N_2O). In this analysis scheme, NO_2 is detected with low sensitivity due to its unfavorable fragmentation behavior in the mass spectrometer. However, test experiments with a different analysis scheme including UV analysis for NO_2 and nondispersive IR-photometric analysis for NO indicated that NO_2 was not formed in significant amounts under the reaction conditions employed. This is confirmed by the fact that in our catalytic runs C and N balances of $100 \pm 5\%$ were routinely obtained in the product analyses.

3. Results and discussion

3.1. Structure of indium species in and on ZSM-5—summary of previous information

The available information about the In-ZSM-5 catalysts employed in this study may be summarized as follows ([28]; cf. Table 1):

3.1.1. Preparation by ion exchange

Materials prepared by aqueous ion exchange at the natural pH of the $In(NO_3)_3$ solution (**IE** (pH nat), but also **IE** (pH 6)) contain both extrazeolite and intrazeolite indium species. The extrazeolite species have a short-range order of $In(OH)_3$. The intrazeolite species are coordinated to six oxygen atoms at 2.12 Å, three more at 3.55 Å, and two Si atoms at 4.02 Å. This coordination was not changed after the thermal treatments mentioned above, most likely due to rapid readsorption of moisture prior to the measurements. No attempt was made to discriminate a short In–O distance that may be expected for the InO^+ ions discussed in the literature [10]. The intrazeolite indium is enriched near the external surface of the zeolite. Precipitation of additional indium changes the relation between extra- and intrazeolite species. While it is obvious that the quantity of extrazeolite species will increase, it is also possible that some additional intrazeolite entities are formed during thermal activation in He by reductive solid-state ion exchange, which may be induced by ammonia adsorbed during precipitation. During the thermal treatments, the extrazeolite indium species form defective In_2O_3 aggregates.

Ion exchange at acidic pH produces exclusively intrazeolite indium species, the structure of which apparently differs from that of intrazeolite species formed at near-neutral pH. This is obvious for the catalyst prepared at pH 2.5, where the indium was coordinated by three oxygen atoms at 2.07 Å and three at 2.19 Å, while more signals of oxygen were detected at higher distances (2.49 and 3.13 Å, with coordination numbers around 1). The EXAFS spectrum of **IE** (pH 1.5) was too noisy for reliable analysis. There was, however, XPS evidence for proceeding dealumination (cf. the XPS Si/Al ratios in Table 3), which suggests that the structure of the indium phase may be even different from that in **IE** (pH 2.5).

3.1.2. Direct precipitation

The direct precipitation route (example **P(H)**), which suffers from poor reproducibility, was found to result in coexisting intra- and extrazeolite indium species. The latter have the short-range order of $In(OH)_3$ and form defective In_2O_3 aggregates after thermal treatment; the structure of the former was not well reproducible. The intrazeolite indium species are enriched in the near-surface region; they may be formed already in the wet step, but additionally during thermal treatment (in particular in inert gas). There are indications that oligomeric intrazeolite InO_x clusters, which were detected by EXAFS in materials prepared by reductive

solid-state ion exchange of excess In_2O_3 in H_2 (with subsequent calcination in air), are also present in the near-surface regions of samples obtained by direct precipitation with subsequent activation in inert gas [28].

3.1.3. Dry routes with $InCl_3$

Interaction of $InCl_3$ with H-ZSM-5 by solid-state ion exchange or by sublimation led to samples containing exclusively intrazeolite indium. Despite considerable risks in the analysis of the first coordination sphere, made up of oxygen and chlorine ([28,34]); see also below) it could be demonstrated that indium was found to be coordinated by ≈ 3.5 O atoms at 2.16 Å, ≈ 2.5 Cl atoms at 2.36 Å, and an additional light scatterer (O or Si) at ca. 2.85 Å in all cases. Washing did not leach indium from these samples, but the stability of the In–Cl bonds depended on the indium content: In a sample with moderate indium content (**SSIE**(4)) chlorine was removed to a significant extent, but not completely, while in the fully loaded **S** sample the coordination sphere remained unchanged after washing.

Published information about samples prepared from $InCl_3$ is limited to the as-prepared and washed states, although further loss of chlorine may be anticipated under conditions typical for catalysis. In the following, the behavior of the intrazeolite InO_xCl_y entities under thermal stress will be described and structural investigations of samples obtained by the transport reaction will be reported.

3.2. Characterization studies

Figure 1a reports the Fourier-transformed EXAFS spectra (absolute part) of samples obtained by solid-state ion exchange (**SSIE**(4)) and by sublimation (**S**) after different treatments and compares them with those of reference compounds—anhydrous $InCl_3$ and the same $InCl_3$ after contact with the ambient atmosphere. It can be seen that there is no order beyond the first shell in the **SSIE**(4) sample irrespective of the treatment (the spectrum obtained after washing, i.e., (**SSIE**(4)/W), was similar and has been omitted). Analogously, the material obtained by sublimation exhibits only two hardly significant scattering contributions beyond the first shell, which are enhanced neither by calcination nor by washing (the latter not shown in Fig. 1a). Calcination after washing, however, resulted in scattering contributions between 3 and 4 Å (uncorrected), at distances typical of In_2O_3 (see inset in Fig. 2). Pronounced long-range order was found in anhydrous $InCl_3$. Contact with the ambient atmosphere destroys this order and shifts the first shell to lower distances, which indicates the introduction of some oxygen into the coordination sphere.

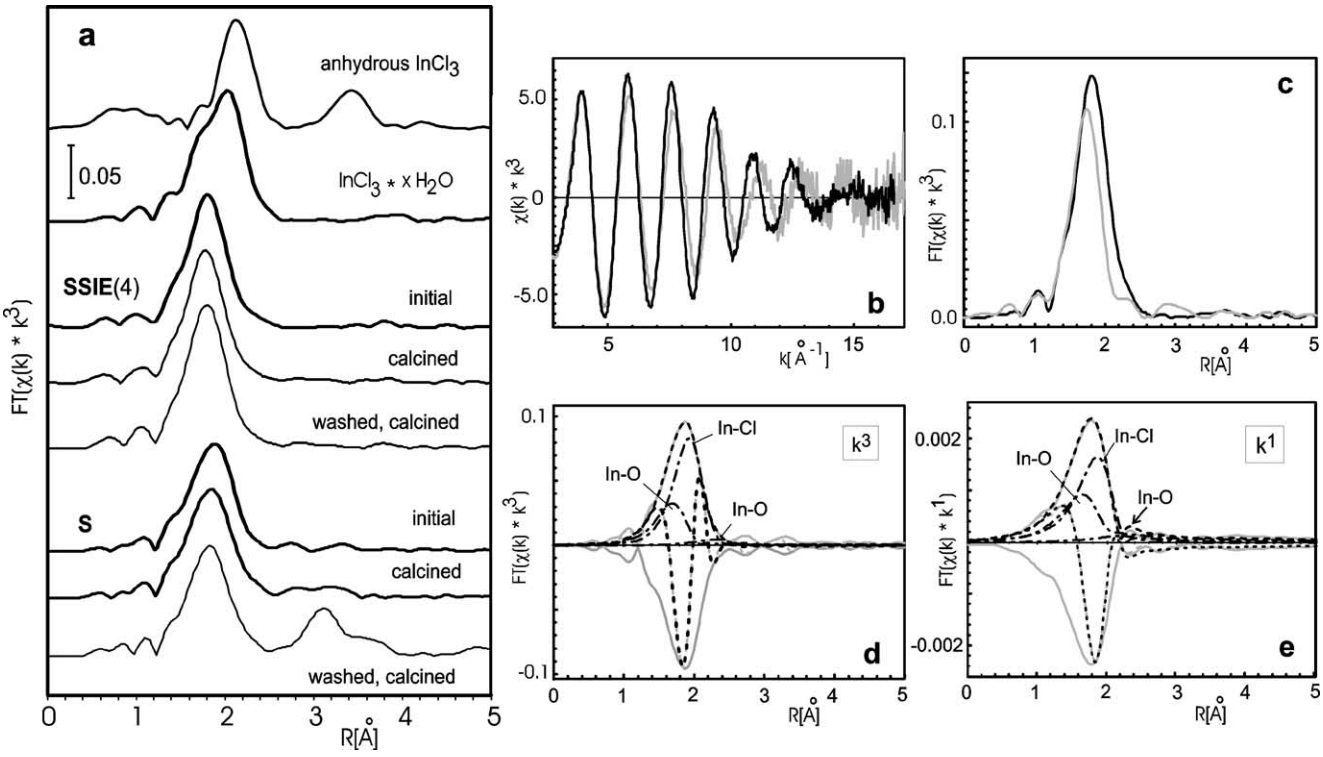

Fig. 1. EXAFS study of the stability of In–Cl bonds in In-ZSM-5 catalysts prepared from the indium source $InCl_3$. (a) Spectra (module of Fourier-transform of k^3-weighted spectra) of reference compounds, of **SSIE**(4) after preparation and after calcination (without and with previous washing in water), and of **S** after preparation and after calcination (without and with previous washing in water). (b and c) Influence of a thermal treatment in flowing humid inert gas: black traces, **SSIE**(3) after preparation; gray traces, **SSIE**(3) after 1 h in flowing helium (2 vol% H_2O) at 623 K. (b) k-space spectra. (c) Module of Fourier-transform of k^3-weighted spectra. (d and e) Identification of scatterers by comparison of the k^3- and k^1-weighted Fourier-transformed EXAFS spectra (example: **S**, as prepared). (d) k^3-weighted. (e) k^1-weighted.

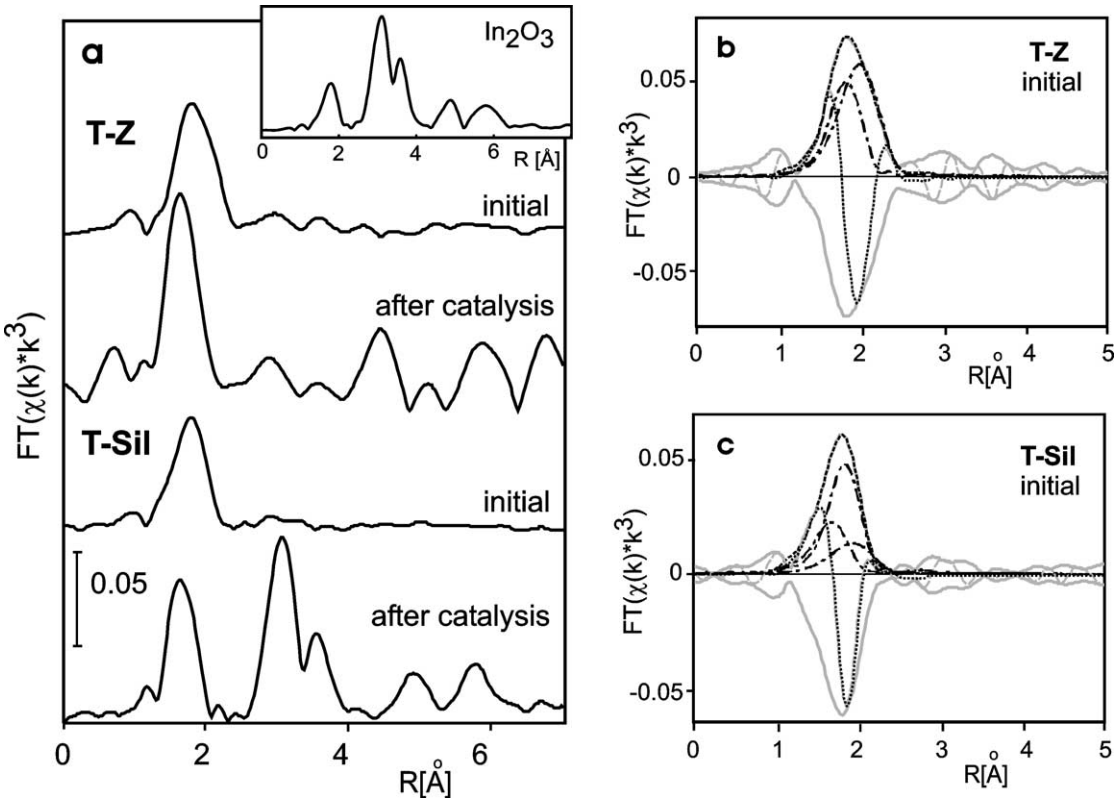

Fig. 2. EXAFS spectra of In–MFI samples prepared by transport reaction between $InCl_3$ and H-ZSM-5 (**T-Z**) or silicalite (**T-Sil**). (a) Spectra (module of Fourier-transform of k^3-weighted spectra) in the as-prepared state and after thermal stress by use in the SCR reaction. (b and c) Examples of the spectral analysis (for parameters see Table 2): (b) **T-Z** in the as-prepared state, (c) **T-Sil** in the as-prepared state.

In the absolute part of the Fourier transformation (FT) shown in Fig. 1a, differences between the spectra are often hardly visible, and they are, indeed, absent in some cases (cf. Table 2). Where the numerical analysis proves differences in the composition of the first coordination sphere, these are clearly discernible in the k-space spectra as demonstrated in Figs. 1b and 1c with the example of **SSIE**(3) [as prepared and after a 1-h treatment in flowing humid He (2 vol% H_2O) at 623 K]. Even if a difference in the absolute part of the FT is absent, the imaginary part (not displayed in Figs. 1a and 1c) will reflect the differences that are seen in the k-space.

The analysis of the first coordination sphere with O and Cl neighbors turned out to be challenging because there were numerous fictitious solutions without physical sense. The presence of chlorine is best demonstrated by comparing the spectra with different k-weightings (k^3 and k^1; see Figs. 1d and 1e): With chlorine present, the different ratios of Cl and O contributions with changing k-weight result in significant modifications of the signal shape. At the same time, an additional contribution of a light scatterer (O or Si) is clearly discerned (only) in the k^1-weighted spectrum (see arrow). It was identified with O in our fits since it occurred also in $InCl_3$ after contact with the ambient atmosphere, but it cannot be excluded that it originated from a Si neighbor in the zeolite samples. Only when this contribution was included were stable solutions obtained for the spectra reported in Fig. 1 (for more details about the fitting procedure cf. [28,34]). The data given in Table 2 were extracted from fits of k^3-weighted spectra, but confirmed after k^1-weighting. Nevertheless, due to the complications indicated, the coordination numbers obtained are subject to considerable uncertainty and represent only general trends.

Table 2 compares the indium coordination spheres as derived from the EXAFS spectra of the catalysts with those of reference compounds (cf. Figs. 1 and 2). Remarkably, in the $InCl_3$-derived In-ZSM-5 catalysts, the coordination sphere around indium is very similar to that found in $InCl_3$ after contact with the ambient atmosphere, but significantly suppressed. There are 2–3 Cl atoms and 3–4 O atoms around indium; in addition, there is a light scatterer (probably O) at a higher distance. As mentioned in [28], In–Cl coordination numbers > 2 are not necessarily erroneous, though it should be expected that $InCl_2^+$ species are deposited by interaction of $InCl_3$ with Brønsted sites. However, at the high temperatures employed in the preparation the interaction may also occur with Lewis sites, which might coordinate $InCl_4^-$ moieties.

Thermal stress and moisture have a different influence on the indium coordination sphere in the catalysts studied. At moderate and high indium content (**SSIE**(4) and **S**, with 4 and 11.8 wt% In, respectively), calcination in air at 823 K leaves the materials unchanged (Fig. 1a, Table 2). The results of the attempt to hydrolyze the In–Cl bond by washing in

Table 2
Influence of treatments on the In coordination in In-ZSM-5 prepared from $InCl_3$: Analysis of In-K EXAFS spectra (cf. Figs. 1 and 2)

Sample, treatment	In–O *R* [Å]/CN	In–Cl *R* [Å]/CN	In–O[a] *R* [Å]/CN	In–X *R* [Å]/CN	In–X *R* [Å]/CN
SSIE(4), initial	2.16/3.4	2.36/2.6	2.86/0.9	–	–
SSIE(4), calcined[b]	2.14/2.8	2.37/3.2	$2.86/0.9_5$	–	–
SSIE(4), washed	2.16_5/5.1	2.39/0.9	2.86/0.7	–	–
SSIE(4), washed/calcined[b]	2.16/4.2	2.35_5/1.8	2.86/0.7	–	–
SSIE(3), initial	2.16/3.8	2.37/2.2	2.86/0.8	–	–
SSIE(3), 2% H_2O/He, 623 K	2.14/5.2	2.35/0.8	2.86/0.7		
S, initial	2.16/3.3	2.37/2.7	2.82/1.1	–[c]	–
S, calcined[b]	2.15_5/3.6	2.38/2.4	2.82/1.2	–[c]	–
S, washed	2.15/3.7	2.37/2.4	2.82/1.0	–[c]	–
S, washed/calcined[b]	2.15/3.6	2.37/2.4	2.82/1.2	**In**: 3.34/0.7	**In**: 3.84/0.5
T-Z, initial	2.19/2.7	2.43/3.3	–	–	–
T-Z, after catalysis	2.10/3.9	–	2.53/2.1	–	–
T-Sil, initial	2.19/1.2 2.22/2.8	2.41_5/1.2	–	–	–
T-Sil, after catalysis[d]	2.13/5.7	–	–	**In**: 3.36/2.2	**In**: 3.83/1.4
$InCl_3$, anhydrous		2.52/4.4		**Cl**: 2.71/1.6	**In**: 3.69/1.5
$InCl_3$, ambient atmosphere	2.20/3.3	2.44/2.7	2.91/0.6	–	–
In_2O_3[e]	2.17/6	–	–	**In**: 3.36/6	**In**: 3.84/6

[a] Si neighbors gave fits of comparable quality.
[b] 823 K, 2 h, synthetic air.
[c] Weak features at 3.2–3.7 Å caused by light scatterers (O or Si).
[d] Additional shell: In–O at 4.0 Å, CN 2.8.
[e] Additional shell: In–O at 4.1 Å, CN 2.5.

water strongly depended on the indium content: While no influence of the water treatment could be detected in **S**, the Cl coordination number decreased significantly in **SSIE**(4), indicating partial hydrolysis of the $InCl_xO_y$ structures. This is also confirmed by the XPS results shown in Table 3, where the Cl/In ratio of **SSIE**(4) decreased significantly upon washing without any change of the In $3d_{5/2}$ binding energy of >446 eV, which is indicative of intrazeolite location of indium [11,28]; i.e., it was not possible to extract all chlorine from the In coordination sphere. Likewise, a treatment in humid inert gas at 623 K (here with **SSIE**(3): Figs. 1b, 1c, Table 2) resulted in only partial hydrolysis of the In–Cl bonds: The In–Cl coordination number decreased significantly, but not to zero. Again, there were no further changes upon subsequent calcination [34].

Surprisingly, in the highly loaded **S** sample, calcination after washing led to a different result than calcination without washing: In the first case, there was clear evidence for an (extrazeolite) In phase, probably with the short-range order of In_2O_3 (Fig. 1a, Table 2). This result should be related to the observation of a minor InO_x phase on the surface of **S** by XPS right after the preparation (Table 3, In signal at 444.8 eV). This phase is not detected by EXAFS, due either to its low amount or to its high defectiveness. The fact that mere calcination is not sufficient to make this phase visible in EXAFS supports the assumption that the oxide phase is a minor constituent, since calcination usually produces In oxide phases from ill-defined oxide or hydroxide precursors (see Ref. [28]). It appears therefore that in the highly loaded **S** sample, washing hydrolyzed $InCl_xO_y$ species loosely held on sites of the near-surface region of the zeolite crystal, where they could aggregate upon subsequent calcination. The amount of the InO_x phase with In_2O_3 short-range order is too low to cause a significant change in the composition of the first indium coordination shell averaged over the whole sample. At lower indium content, all indium is coordinated to sites that provide more stability to the $InCl_xO_y$ structures; hence, no detachment and aggregation is noted.

Figure 2 and Tables 2 and 3 summarize characterization results obtained with the samples prepared by transport reaction between H-ZSM-5 or silicalite-1 and $InCl_3$. The In $3d_{5/2}$ XPS binding energies measured with these ma-

Table 3
XPS binding energies and elemental ratios of In–MFI materials

Sample	BE (In $3d_{5/2}$), eV	In/Si		Cl/In	Si/Al[a]
		XPS	Bulk		
IE (pH 6)	445.0 85% 446.2 15%	0.074	0.0057	–	16.9
IE (pH 2.5)	446.1_5	0.0048	0.0013	–	15.4
IE (pH 1.5)	446.0_5	0.0015	0.0009	–	22.5
SSIE(4)	446.2	0.014	0.024	1.8	12.4
SSIE(4)/W	446.4	0.014	0.024	0.7	16.4
S	444.8 15% 446.0 85%	0.027	0.070	1.8	11.9
T-Z	445.7	0.006	0.002	4.2	6.5
T-Sil	445.9	0.033	0.008	2.0	–
In_2O_3	444.0_5				
$InCl_3$[b]	446.3			2.5	

[a] Parent zeolite: initial NH_4 form, $(Si/Al)_{XPS} = 10$; after treatment in 0.025 m HNO_3 for transfer into H form, $(Si/Al)_{XPS} = 17$.
[b] After contact with the ambient atmosphere.

terials (Table 3) are near 446 eV and therefore indicative of intrazeolite indium. In **T-Z**, this binding energy is, actually, rather low (445.7 eV), but this can be ascribed to the presence of In(I) in significant amounts as disclosed by the localization of the In *K*-edge in XAFS [34]. The chlorine content of the near-surface region of **T-Z** was extraordinarily large (cf. Cl/In ratio from XPS in Table 3); at the same time a considerable surface enrichment of Al was noted ($(\mathrm{Si/Al})_{\mathrm{XPS}} = 6.5$). Probably, the prolonged contact with HCl at 673 K has led to partial dealumination of the H-ZSM-5, with chlorided extralattice Al species deposited in the external surface region.

The EXAFS spectra shown in Fig. 2 confirm that indium is exclusively intrazeolite after the preparation via transport reaction. There is no order at higher distances, and the first coordination sphere consists of Cl and O (Table 2). Remarkably, this is also the case in **T-Sil**, and the rather high oxygen content of the indium coordination sphere indicates an interaction of the $InCl_3$ with the silicalite matrix, probably via the silanol groups. After thermal stress (here by use in the SCR reaction) the first shell becomes very narrow in **T-Z** (Fig. 2). There are no significant scattering events around 3 Å (uncorrected) that could be ascribed to indium neighbors, while the maxima at higher distances are due to an experimental problem. The analysis (Table 2) shows that there is no more Cl in the indium coordination sphere. The structure of this coordination sphere differs significantly, however, from that found in samples prepared in aqueous media (**IE** (pH 2.5), with 3 O at 2.09 Å and 3 O at 2.19 Å, internal phase of **IE** (pH 6) with 6 O at 2.12 Å, vide supra). A scatterer at 2.51 Å is assigned to O although an alternative assignment to Si cannot be completely ruled out on the basis of the experimental spectrum. In **T-Sil**, however, the signature of In_2O_3 is clearly seen after catalysis. The enhanced intensity of the first coordination sphere (reflected in low CN of the In–In spheres at 3.36 and 3.83 Å) shows, however, that the InO_x clusters coexist with a highly disperse In phase.

In summary, the preparations used in this study provide three kinds of indium sites: isolated intrazeolite oxo species, isolated intrazeolite $InCl_xO_y$ species, and extrazeolite aggregates, which have the short-range order of In_2O_3 after calcination. Exclusively intrazeolite In oxo species were obtained by ion exchange at low pH and by transport reaction with subsequent thermal stress (**T-Z** after catalysis). Coexisting intra- and extrazeolite species were obtained by ion exchange with accidental or intentional precipitation (**IE** (pH 6), **IE** (pH nat), **IE-P**). The coordination geometry of the intrazeolite In species formed under the various conditions (pH 6, 2.5, transport reaction + thermal stress) are all different. This should extrapolate also to the sample **IE** (pH 1.5), where reliable EXAFS analysis was not possible. Intrazeolite $InCl_xO_y$ species result from sublimation and solid-state ion exchange with the indium source $InCl_3$. Because of the observed stability trends of the In–Cl bond, the indium coordination sphere will remain highly chlorided during catalysis when the indium content is intermediate or large (**SSIE**(4), **S**), but should lose chlorine at low indium content (e.g., **SSIE**(1)). Partial loss of chlorine was also effected by washing a sample of intermediate indium content (**SSIE**(4)) in water.

3.3. In-ZSM-5 of different preparation: catalytic behavior in the SCR with methane

Figure 3 reports typical features of the catalytic behavior of In-ZSM-5 catalysts in the SCR of NO with methane, as found in our investigations. NO and methane conversion data from different preparations are summarized in panels a and b and compared with that of H-ZSM-5. The NO conversions are not very attractive, but it should be kept in mind that the merit of the In-ZSM-5 system is rather its susceptibility to promotion than its intrinsic activity. With the ion-exchanged In-ZSM-5 (**IE** (pH nat)), the NO conversion peaked at 673 K ($X(\mathrm{NO})_{\max} = 39\%$), but a considerable improvement was achieved by precipitating additional indium onto the external surface (**IE-P**, $X(\mathrm{NO})_{\max} = 51\%$). A catalyst made by mere precipitation (**P(H)**) showed less favorable behavior, with a peak conversion of only 31% at 723 K. On the other hand, it is possible to induce significant SCR activity even by mere mechanical mixing of the zeolite with an indium compound: With $\mathbf{MM}_{\mathrm{N,Hy}}$, NO conversions higher than those obtained with H-ZSM-5 were measured in a wide temperature range, with a peak conversion of 35% at 773 K. However, with a mixture, in which care was taken to avoid the presence of reducing agents as NH_4 ions ($\mathbf{MM}_{\mathrm{H,O}}$), there was hardly any excess activity beyond that of H-ZSM-5 (not shown in Fig. 3).

The methane conversions found confirm that In-ZSM-5 is a system that utilizes the reductant well: With **IE** (pH nat), the peak NO conversion of almost 40% was obtained with a methane conversion of only 23%. After additional precipitation of indium (**IE-P**), the methane activation activity increased significantly, in particular at $T > 700$ K.

Figure 3 also summarizes the poisoning influence of water and Na ions on the SCR activity, which was studied with the samples **IE** (pH nat) and **P(H)**. The presence of 2 vol% of water in the feed strongly suppressed the SCR activity of these In-ZSM-5 catalysts, in particular at low temperatures. The influence is stronger with **P(H)** than with **IE** (pH nat). When the non-calcined precursor was back-exchanged with Na ions by stirring in a 1 mol/l $NaNO_3$ solution, the NO conversions in dry feed were also strongly attenuated, far below those obtained with H-ZSM-5. Remarkably, the methane activation activity also strongly suffered from Na poisoning.

While these data illustrate the diversity of phenomena to be observed with In-ZSM-5 catalysts, it is obvious that they result from materials that contain intra- and extrazeolite indium species in unknown proportions. For **IE** (pH nat), **IE-P**, and **P(H)**, this is clear from [28] (cf. Table 1a) and the coexistence between extra- and intrazeolite indium in **P(H)**

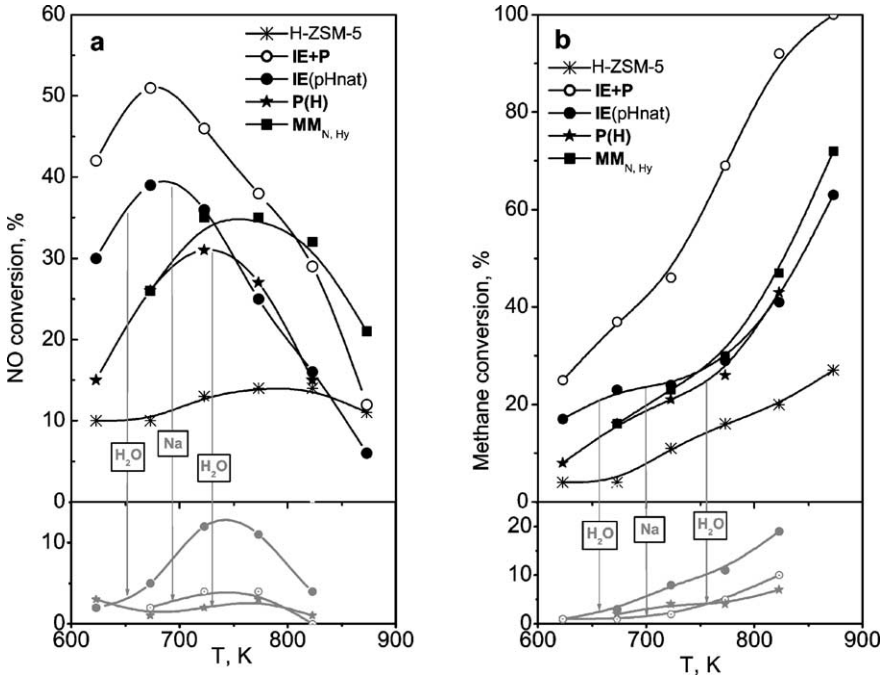

Fig. 3. Catalytic behavior of In-ZSM-5 catalysts of different preparations in the SCR of NO by methane (1000 ppm NO, 1000 ppm methane, 2% O_2 in He, 30,000 h^{-1}); (a) NO conversion. (b) Methane conversion: preparations compared are ion exchange without pH control (**IE** (pH nat) (●); in the presence of 2 vol% H_2O (◉); after back-exchange with Na^+ (⊙); the same with subsequent precipitation of indium from supernatant solution (**IE** + **P**) (○); precipitation of indium onto H-ZSM-5 by ammonia (**P(H)** (★); in the presence of 2 vol% H_2O (★); and mechanical mixture NH_4-ZSM-5/$In(OH)_3$ (■).

is also illustrated by a TPR profile obtained with a parallel preparation, which is given in Fig. 6b. In the $\mathbf{MM}_{N,Hy}$ mixture, it may be assumed that reductive solid-state ion exchange induced by NH_3, which is evolved from NH_4-ZSM-5 during thermal activation, had occurred to some extent, similarly to the processes observed with precipitate catalysts. In $\mathbf{MM}_{H,O}$, the probability of indium introduction into the zeolite would be considered to be lowest although it has been reported that solid-state ion exchange can proceed under the activation conditions [11], most likely following an autoreduction of the In(III) oxide [35].

To identify the structural catalyst features that cause the various effects to be observed in Fig. 3, it would be desirable either to have samples that contain exclusively extra- or intrazeolite indium species or to be able to control the amounts of these species. From the characterization results reported above it is obvious that the intentional preparation of In-ZSM-5 with particular properties is difficult. Thus, we have not yet succeeded in making a series of In-ZSM-5 containing a particular indium species (i.e., with identical coordination sphere) in varying amounts, from which a clearcut assignment of catalytic properties and a quantitative assessment of intrinsic activities could be made. Nevertheless, it will be seen that the materials prepared in the present study form a basis that already makes it possible to derive some relevant conclusions about the sites involved in the SCR reaction.

NO and methane conversions of In-ZSM-5 catalysts with exclusively intrazeolite In oxo species (**IE** (pH 2.5), **IE** (pH 1.5), **T-Z**) are given in Fig. 4 and compared with conversion data from catalysts with coexisting extra- and intrazeolite indium species on the basis of a zeolite (**IE** (pH 6)) and of silicalite-1 (**T-Sil**). As expected, intrazeolite In oxo species are active sites for the SCR reaction, but Fig. 4 reveals some more relevant trends. Thus, there is no clear correlation between the NO conversions and the indium content of the samples. A linear decrease at all temperatures would be expected between (**IE** (pH 2.5) and **IE** (pH 1.5) if their indium sites were identical, just of different abundance. Instead, there is a shift of the NO conversion curve to higher temperatures so that **IE** (pH 1.5) even exceeds **IE** (pH 2.5) at 773 K. Analogously, **T-Z**, which contains the most indium, has the lowest activity, with a NO conversion curve strongly shifted to higher temperatures. These shifts can be, certainly, ascribed to the effects of the acidic conditions encountered by the zeolites during the preparation. It is, however, less straightforward to identify the operating mechanism in more detail. The acidic conditions lead to changes of the indium coordination sphere (vide supra) and to dealumination tendencies (cf. Table 3). We believe that the shift of the NO conversion curve is primarily caused by the modification of the indium site: Since acid treatment at pH 1–2 is a standard procedure for transferring Na-ZSM-5 into H-ZSM-5 it is not likely that such treatment could induce a shortage of Brønsted sites that would limit the SCR rate. Such limitation could, however, be an additional reason for the poor performance of **T-Z**.

Those catalysts that contain both extra- and intrazeolite indium species exhibit remarkable differences and similarities: While **IE** (pH 6) provides the highest NO conversion, there is no SCR activity at all with **T-Sil** (Fig. 4). On the

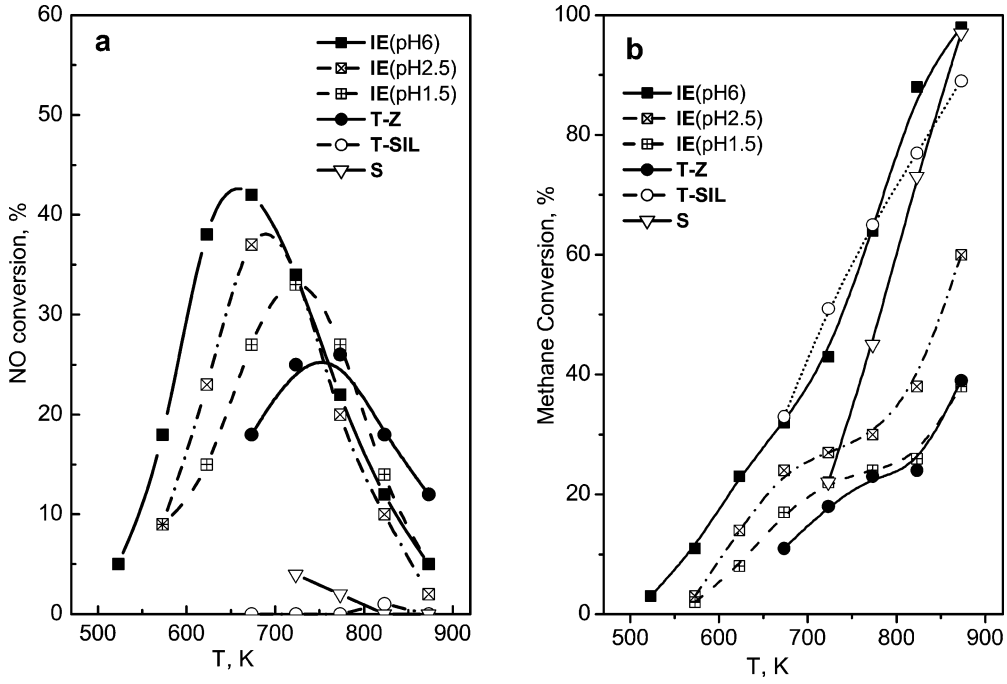

Fig. 4. Catalytic behavior of In-ZSM-5 with exclusively intrazeolite In oxo species (**IE** (pH 2.5), **IE** (pH 1.5), **T-Z**) and with coexisting intra- and extrazeolite In oxo species (**IE** (pH 6), **T-Sil**) in the SCR of NO by methane. Comparison with a catalyst containing intrazeolite $InCl_xO_y$ sites (**S**): (a) NO conversion, (b) methane conversion.

other hand, both catalysts have almost the same methane activation activity. This suggests that the failure of **T-Sil** in the SCR reaction is due to its lack of Brønsted sites.

When the sample **IE** (pH 6) is compared with the remaining In-ZSM-5 materials represented in Fig. 4, it is obvious that no particular contribution of the extrazeolite indium phase can be derived from the NO conversion curve. The trend to higher peak conversions at lower temperatures extrapolates just the tendencies identified before for materials with exclusively intrazeolite indium. However, as mentioned above, the extrazeolite indium can be traced in the methane conversion curves. While that of **IE** (pH 6) rises steeply over the whole temperature range, those of **IE** (pH 2.5), **IE** (pH 1.5), and **T-Z** all level off around 700 K before setting out for a new steep increase at higher temperatures. From this, the particular methane activation activity of **IE** (pH 6) can be assigned to the extrazeolite indium phase, which includes possible bonds between the extrazeolite species and the zeolite surface at the borderline of the aggregates (covalent In–O–Si and In–O–Al bonds). By analogy, the intrazeolite indium in **T-Sil**, which is most likely also bonded via In–O–Si bonds, cannot be excluded as potential methane activation site.

Figure 4 contains also data from a catalyst prepared by sublimation of $InCl_3$ into H-ZSM-5 (**S**). Data from catalysts prepared by solid-state ion exchange of $InCl_3$ into H-ZSM-5 are summarized in Fig. 5. The NO conversions of these catalysts, in which indium is coordinated both to O and to Cl according to our characterization studies, are disappointing. At low indium content (**SSIE**(1), **SSIE**(2)), the NO conversion still exceeds that of H-ZSM-5, with a peak NO conversion of 25% at 673 K. With increasing indium content, the NO conversions become lower than those measured with the parent zeolite. The NO conversion curve of catalyst **S** is almost identical to that of **SSIE**(4) (Figs. 4 and 5). At the same time, these samples are quite active for methane activation. It may be observed, however, that the methane conversion increases significantly between **SSIE**(1) and **SSIE**(2), but only marginally at further increase of the indium content. Again, the methane activation activity of material **S** is close to that of **SSIE**(4). Figure 5 shows also the effect of the washing procedure on the catalytic properties of **SSIE**(4): There is a significant enhancement in both the NO and the methane conversions.

The activity data of these catalysts can be discussed by reference to the chlorine content of the indium coordination sphere as revealed by the characterization studies. It appears that highly chlorided indium species are not active for the SCR reaction but capable of activating methane. This (unselective) methane activation does not require Brønsted sites because it occurs on catalysts with strongly varying concentrations of the latter (**S**, **SSIE**(4); see IR data in [28,34]). It will be shown in part II of this paper [27] that it forms the basis of appreciable SCR activity observed upon addition of a promoter that provides a sufficient NO_2 supply. Upon increasing oxygen content in the indium coordination sphere, both the SCR and the methane activation activity of the (unpromoted) $InCl_xO_y$ species increase (compare **SSIE**(4) and **SSIE**(4)/W activities in Fig. 5, coordination spheres in Table 2). The same trends may explain the

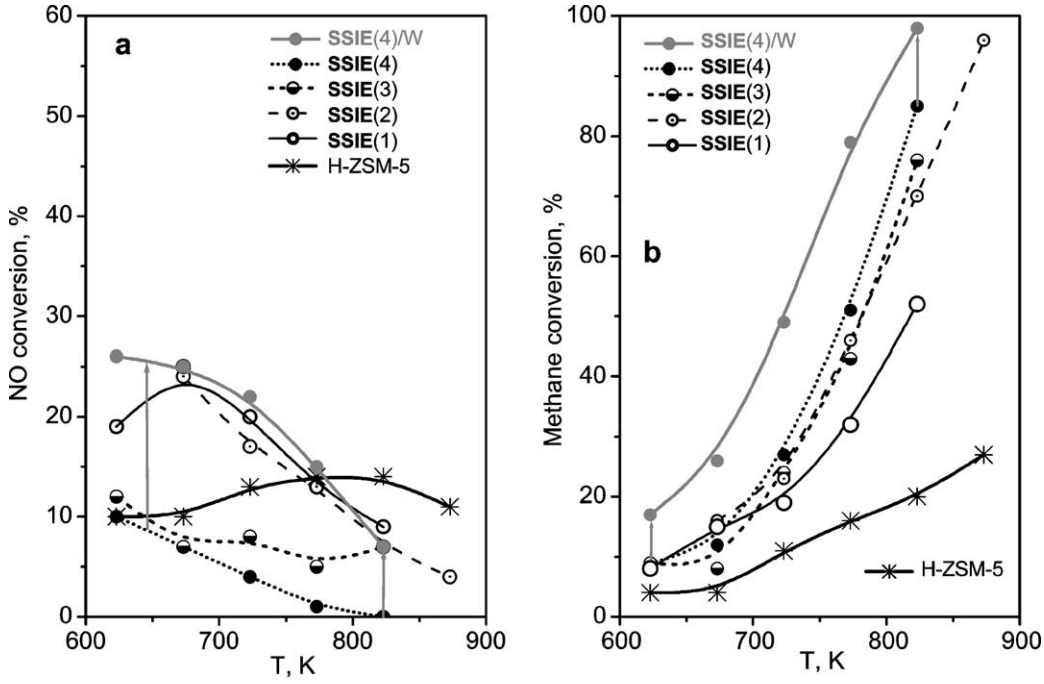

Fig. 5. Catalytic behavior of In-ZSM-5 with intrazeolite $InCl_xO_y$ species. Influence of indium content and of a washing step during the preparation. For conditions see legend to Fig. 3. (a) NO conversion, (b) methane conversion.

increase of the SCR activity at smaller indium contents. Although the In coordination spheres did not differ in the freshly prepared catalysts **SSIE**(1) through **SSIE**(4), that of **SSIE**(1) should contain less chlorine after catalysis than that of **SSIE**(4) because of the higher stability of the In–Cl bonds at higher indium content.

In summary, it was found that intrazeolite In oxo species are active sites for the SCR of NO by methane while the presence of chlorine has an adverse effect on the SCR activity. $InCl_xO_y$ sites are, however, capable of methane activation, in particular at $T \geqslant 700$ K. High methane activation activity is also observed in the presence of extrazeolite indium phases.

3.4. Studies with mechanical mixtures

The observation of SCR activity with the mechanical mixture $\mathbf{MM}_{N,Hy}$ (Fig. 3) may suggest that there are also extrazeolite indium sites that support the SCR reaction at an attractive rate. However, because of the significant tendency of indium to undergo reductive and autoreductive solid-state ion exchange [11,35]), the formation of intrazeolite indium species as observed with catalysts made by precipitation of $In(OH)_3$ on the zeolite cannot be ruled out. Because proximity between the zeolite and the indium source should be crucial for (auto)reductive solid-state ion exchange to proceed to an appreciable extent, this proximity was varied deliberately to prepare a set of mechanical mixtures with varying content of intrazeolite indium species (mixtures $\mathbf{MM}_{N,Hy}$ (A), (B), and (C); cf. "Experimental," Table 1). In mixture A, there was no close proximity at any stage of the preparation and during catalysis because the zeolite and the indium component (In_2O_3 after activation) were segregated into separate pellets at any time. In mixture C, the components were always near to each other because the starting materials NH_4-ZSM-5 and $In(OH)_3$ were pelletized together. In mixture B, these components were separated during the evolution of NH_3 from NH_4-ZSM-5, i.e., the reductant that might induce reductive solid-state ion exchange, but close to each other in the remaining steps including thermal activation in helium. Hence, in mixture B the tendency to formation of intrazeolite indium species was expected to be intermediate between mixtures A and C. Temperature-programmed reduction was employed to verify these expectations.

Figure 6a shows the catalytic results obtained with these mixtures. As expected, mixture A is inferior to mixtures B and C which, on the other hand, exhibit identical catalytic behavior, with a higher peak NO conversion achieved at a lower temperature than with mixture A. The performance of mixtures B and C is comparable with those of the best In-ZSM-5 catalysts reported in this paper with the exception of **IE-P**. Remarkably, the conversion-temperature curves shown for $\mathbf{MM}_{N,Hy}$ in Fig. 3 were not reproduced by any of the mixtures $\mathbf{MM}_{N,Hy}$ (A), (B), or (C) made of the same constituents.

The TPR profiles of these mixtures after catalysis (and reoxidation in air), which are shown in Fig. 6b, reveal that the expectations concerning the numbers of intrazeolite indium sites have been fulfilled only to a very limited extent. Unlike the reference TPR profile taken from a parallel preparation of **P(H)**, the profiles of the mechanical mixtures exhibit

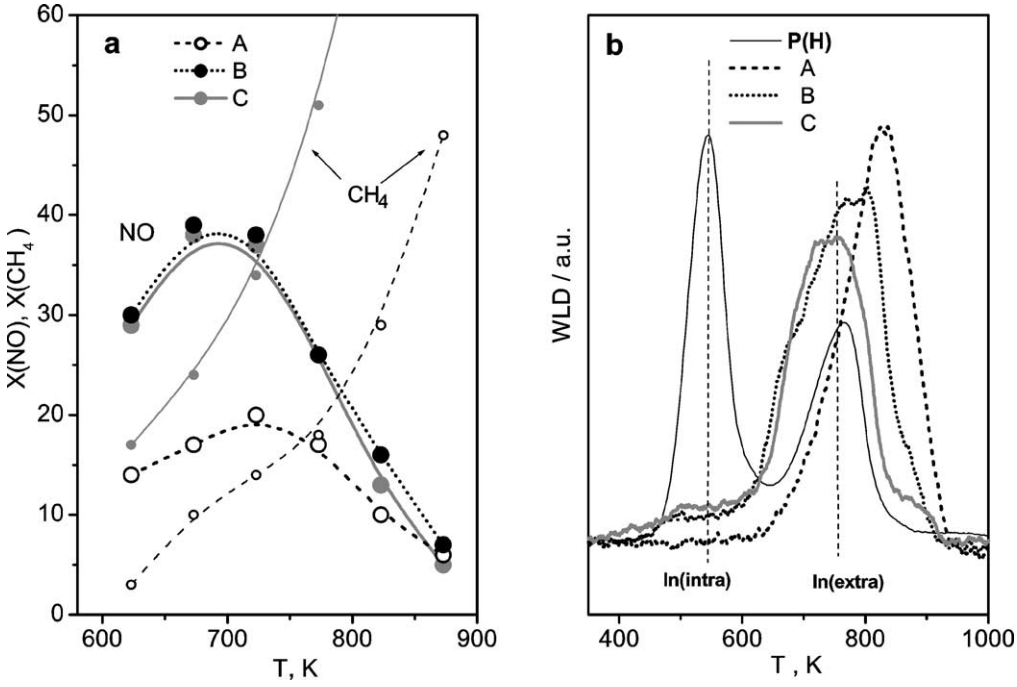

Fig. 6. SCR with mechanical mixtures of an indium compound with H-ZSM-5. (a) NO and methane conversions, (b) TPR traces (A, B, and C based on identical indium content in the sample). (A) NH_4-ZSM-5 and $In(OH)_3$ pressed and activated in separate pellets ("segregated mixture"); (B) as mixture A, but then crushed and repelletized in pellets containing both indium and zeolite, (C) NH_4-ZSM-5 and $In(OH)_3$ pressed together in pellets before activation and used in this form.

only one peak, however, with asymmetries and shoulders. Mixture A has no intensity at all in the temperature region typical of intrazeolite indium sites [25,36] and the profile peaks at a temperature significantly higher than for the signal of extrazeolite indium sites. This may be explained by a weak interaction between In_2O_3 and the H-ZSM-5: It has been shown in [14,36] that the peak reduction temperature of In_2O_3, which was $\approx$870 K under similar conditions, decreases significantly when the oxide is mixed with an acidic zeolite as H-ZSM-5. A similar effect has been reported for the Fe_2O_3/H-ZSM-5 system [8]. In Fig. 6b, it can be seen that mixture B produced a very small low-temperature signal, actually a shoulder, which contributes not more than 5% to the total signal area. From this, the In/Si ratio for the intrazeolite species is on the order of 0.002, i.e., well comparable with **IE** (pH 2.5) and **IE** (pH 1.5). The center of the high-temperature peak is in the region where the signal of extrazeolite In oxide species is expected, but there are excursions at higher and at lower temperatures. The former, which should represent In_2O_3 in bad contact with the zeolite, is not surprising for a mechanical mixture even if prepared by grinding together the constituents. The shoulder at 680 K is not easy to assign. Extending the trend between intensity of In–zeolite interaction and peak reduction temperature, it could be ascribed to an extrazeolite site with a particular bond to the surface. In the trace of mixture C, the center of the main peak is still more shifted to lower temperatures, and the amount of intrazeolite indium species seems to be further increased. The difference to mixture B is, however, not as pronounced as would have been expected from the conditions set to encourage reductive (C) or merely autoreductive (B) solid-state ion exchange.

From these observations, it appears that intrazeolite indium formed by solid-state ion exchange phenomena (reductive via NH_3 or autoreductive) may be responsible for the extra activity exhibited by the nonsegregated mixtures $\mathbf{MM}_{N,Hy}$ (B) and (C). This assignment is, however, not without doubt because the increased amount of intrazeolite indium in mixture (C) is not at all reflected in the NO conversions. Particular interactions between the zeolite and the extrazeolite indium aggregates could also contribute to the increased activity of these mixtures because the close proximity was a critical condition for the higher NO conversions. Such sites, which should include covalent In–O–Si or In–O–Al bonds, cannot be discriminated from the TPR profiles so far. At the present stage, it cannot be excluded that there is also a significant contribution to the effect of proximity between indium and zeolite components from a minimization of diffusion paths in a bifunctional mechanism, in which a volatile intermediate released by extrazeolite indium sites has to find zeolite Brønsted sites to be converted to nitrogen, carbon oxides, and water. Such a mechanism has recently been demonstrated for the SCR of NO by methane over CeO_2/H-ZSM-5 catalysts [26] and the bifunctional nature of the SCR reaction over In-ZSM-5 is suggested by several observations in the present study (e.g., Na poisoning, failure of **T-Sil**). Further studies with CeO_2-promoted In-ZSM-5, which will be reported in part II of this series [27], suggest that the extra activity of the nonsegregated mixtures (B) and (C) largely originates from

new sites in the interface between InO_x aggregates and the zeolite surface.

The unexpected differences between the (early) sample $\mathbf{MM}_{N,Hy}$ (Fig. 3) and the (later) mixture $\mathbf{MM}_{N,Hy}$ (C),which were prepared following the same procedure, may serve as an example for open questions remaining with the rather complex In–zeolite catalyst system. While the peak conversions of both mixtures are similar, the earlier sample achieved them at a higher temperature, but exhibited a broader useful temperature region than the later $\mathbf{MM}_{N,Hy}$ (C). The reason for this is not known. In this study, a segregation between extrazeolite InO_x sites and the zeolite (mixture $\mathbf{MM}_{N,Hy}$ (A); cf. Fig. 6a) and framework damage by acidic attack (**IE** (pH 1.5), **T-Z**, in Fig. 4) have been identified as possible reasons for an upward shift of the temperature of peak NO conversion. It is not clear whether one of these influences was operative in $\mathbf{MM}_{N,Hy}$ or if there are other, unidentified reasons for the behavior observed.

4. Conclusions

The catalytic behavior of In-ZSM-5 catalysts in the selective reduction of NO by methane exhibits considerable variations when different catalyst preparations are compared. For a study of relations between the structure of the indium sites and their catalytic properties, In-ZSM-5 materials from different preparations (aqueous ion exchange at different pH values, precipitation; solid-state ion exchange, sublimation and transport reaction with an $InCl_3$ indium source) have been investigated by EXAFS and XPS to select materials with known location of the indium sites (exclusively intrazeolite, coexisting intra- and extrazeolite) and basic features of the indium coordination sphere (exclusively O ligands, O and Cl ligands). In addition, physical mixtures between $In(OH)_3$ and NH_4-ZSM-5 have been studied.

It has been found that intrazeolite indium oxo species are active SCR sites, but their catalytic properties depend on details of the coordination environment. The simultaneous presence of extrazeolite InO_x species adds little to the SCR activity but enhances the methane activation, resulting in increased total oxidation. A catalyst that contains intra- and extrazeolite indium sites on silicalite-1 activates methane without reducing any NO. From this it was concluded that the SCR over In-ZSM-5 requires acidic sites. Intrazeolite InO_xCl_y species possess low SCR activity although they are well capable of activating methane. The SCR activity appears to increase with the O content of the coordination sphere.

Physical mixtures of In_2O_3 and H-ZSM-5 (made from $In(OH)_3$ and NH_4-ZSM-5) exhibit activities similar to those of In-ZSM-5 catalysts prepared by aqueous techniques. These activities are obtained only when the constituents are well mixed in the catalyst pellets, while segregation into separate pellets strongly decreases the NO conversions.

Acknowledgments

Financial support by the Federal Ministry of Education, Science and Technology (BMBF), Grants 03C0271/B6 and 03C0271/A3, is gratefully acknowledged.

References

[1] A. Fritz, V. Pitchon, Appl. Catal. B 13 (1997) 1.
[2] V.I. Parvulescu, P. Grange, B. Delmon, Catal. Today 46 (1998) 223.
[3] Y. Traa, B. Burger, J. Weitkamp, Micropor. Mesopor. Mater. 30 (1999) 3.
[4] M. Shelef, Chem. Rev. 95 (1995) 209.
[5] D. Kaucky, A. Vondrova, J. Dedecek, B. Wichterlova, J. Catal. 194 (2000) 318.
[6] P. Marturano, L. Drozdova, A. Kogelbauer, R. Prins, J. Catal. 192 (2000) 236.
[7] A.A. Battiston, J.H. Bitter, D.C. Koningsberger, Catal. Lett. 66 (2000) 75.
[8] F. Heinrich, C. Schmidt, E. Löffler, M. Menzel, W. Grünert, J. Catal. (2002) in press.
[9] E. Kikuchi, K. Yogo, Catal. Today 22 (1994) 73.
[10] E. Kikuchi, M. Ogura, I. Terasaki, Y. Goto, J. Catal. 161 (1996) 465.
[11] M. Ogura, N. Aratani, E. Kikuchi, Stud. Surf. Sci. Catal. 105 (1997) 1593.
[12] X.J. Zhou, T. Zhang, Z.S. Xu, L.W. Lin, Catal. Lett. 40 (1996) 35.
[13] M. Ogura, T. Ohsaki, E. Kikuchi, Micropor. Mesopor. Mater. 21 (1998) 533.
[14] X.J. Zhou, Z.S. Xu, T. Zhang, L.W. Lin, J. Mol. Catal. 122 (1997) 125.
[15] R. Heinisch, M. Jahn, C. Yalamas, Chem. Eng. Technol. 22 (1999) 337.
[16] T. Maunula, Y. Kintaichi, M. Inaba, M. Haneda, K. Sato, H. Hamada, Appl. Catal. B 15 (1998) 291.
[17] T. Maunula, Y. Kintaichi, M. Haneda, H. Hamada, Catal. Lett. 61 (1999) 121.
[18] E. Kikuchi, M. Ogura, N. Aratani, Y. Sugiura, S. Hiromoto, K. Yogo, Catal. Today 27 (1996) 35.
[19] M. Ogura, M. Hayashi, E. Kikuchi, Catal. Today 42 (1998) 159.
[20] M. Ogura, M. Hayashi, E. Kikuchi, Catal. Today 45 (1998) 139.
[21] X.D. Wang, T. Zhang, X.Y. Sun, W. Guan, D.B. Liang, L.W. Lin, Appl. Catal. B 24 (2000) 169.
[22] B. Sulikowski, J. Janas, J. Haber, A. Kubacka, Z. Olejniczak, E. Wloch, J. Chem. Soc. Chem. Commun. (1998) 2755.
[23] F.-W. Schütze, H. Berndt, T. Liese, T. Sowade, W. Grünert, F. Simon, U. Ströder, DP 10065717.6, December 22, 2000.
[24] F.-W. Schütze, H. Berndt, M. Richter, B. Lücke, C. Schmidt, T. Sowade, W. Grünert, Stud. Surf. Sci. Catal. 135 (2001), A10-O-1.
[25] H. Berndt, F.-W. Schütze, M. Richter, T. Sowade, W. Grünert, Appl. Catal. B, in press.
[26] T. Liese, E. Löffler, W. Grünert, J. Catal. 197 (2001) 123.
[27] T. Sowade, C. Schmidt, E. Löffler, F.-W. Schütze, H. Berndt, W. Grünert, to be published.
[28] C. Schmidt, T. Sowade, E. Löffler, A. Birkner, W. Grünert, J. Phys. Chem. B 106 (2002) 4085.
[29] C.D. Wagner, in: D. Briggs, M.P. Seah (Eds.), Practical Surface Analysis, Vol. 1, Wiley, Chichester, 1990, p. 635.
[30] D.C. Koningsberger, R. Prins, in: J.D. Winefordner (Ed.), Chemical Analysis, Vol. 92, Wiley, New York, 1988, p. 673.
[31] F.W. Lytle, D.E. Sayers, E.A. Stern, Physica B 158 (1989) 701.
[32] T. Ressler, J. Phys. IV France 7 (1997), C2–269.
[33] S.I. Zabinsky, J.J. Rehr, A. Ankudinov, J.C. Albers, M.J. Eller, Phys. Rev. B 52 (1995) 2995.
[34] C. Schmidt, PhD thesis, Ruhr Universität, Bochum, 2001.
[35] M.R. Mihályi, H.K. Beyer, Chem. Commun. (2001) 2242.
[36] M. Richter, H. Berndt, R. Fricke, B. Lücke, in: Proceedings of the Conference on Catalysis on Solid Acids and Bases, Berlin, DGMK, Hamburg, 1996, p. 283.